Neutron scattering study of low doped $La_{2-x}Ba_xCu0_4$ with $0 \leq x \leq 0.025$

G. Van Gastel[1], Z. Yamani[2], J. Carlo[2], B. Gaulin[1]

1 Department of Physics and Astronomy, McMaster University, Hamilton, Ontario, L8S 4M1, Canada

2 National Research Council, Canadian Neutron Beam Centre, Chalk River, ON, Canada

High-temperature superconductivity has been and remains one of the enduring mysteries of modern physics. In particular, the high T_c cuprates have generated a substantial amount of interest over nearly three decades. Within this family of materials, superconducting transition temperatures well above the boiling point of liquid nitrogen (77K) have been found, for example, in $HgBa_2Ca_2Cu_3O_x$, $YBa_2Cu_3O_7$ and $Bi_2Sr_2Ca_2Cu_3O_{10}$.[1][2][3] The first high T_c material, $La_{2-x}Ba_xCuO_4$ (LBCO), discovered by Bednorz and Müller in 1986,[4] demonstrates a number of interesting behaviours across its phase diagram, indicating coupling between magnetic and electronic degrees of freedom.[5] While its sister material, $La_{2-x}Sr_xCuO_4$, has been extensively studied, LBCO has been less studied until relatively recently owing to the difficulty in obtaining high-quality single crystals, a problem which has been remedied over the past decade by the use of the floating-zone image furnace method of crystal growth.

When the Mott insulating parent material, La_2CuO_4, is doped with Ba, the 3D commensurate antiferromagnetic ground state is rapidly killed off leaving an incommensurate, 2D antiferromagnetic structure for $x > 0.02$.[5] Previous studies of these materials have demonstrated that the incommensuration possesses a complex doping dependence.[6] In particular, for low dopings ($0.02 < x < 0.05$) the incommensuration is small and diagonal with respect to the Cu-O-Cu bonds. With increased doping, the incommensuration broadens and at the onset of superconductivity ($x = 0.05$) the orientation rotates to become collinear with the Cu-O-Cu bonds. This type of doping-dependent behaviour indicates that much remains unknown about the relationship between magnetism and superconductivity in the low-doping region of the phase diagram. We have grown several large single crystal samples of $La_{2-x}Ba_xCuO_4$ with Ba^{2+} concentrations of $x < 0.05$ in order to extend previous studies [5][6] to even lower doping levels. Specifically, we have chosen doping levels of $x = 0$, $x = 0.006$, $x = 0.0125$ and $x = 0.025$ in order to explore the magnetic behaviour of underdoped LBCO in the low-doped to undoped region. In addition, we have also grown a high-quality crystal of electron-doped $La_{2-x}Ce_xCuO_4$ (LCCO) with a Ce^{4+} concentration of $x = 0.025$. Despite the change of dopant, high-resolution powder x-ray diffraction has confirmed that the Ce-doped material crystallizes in the same space group, Bmab, and with similar lattice parameters to LBCO. The electron-doped region of the cuprate family phase diagram has been well-studied with materials such as $Nd_{2-x}Ce_xCuO_4$ and $LaPr_{1-x}Ce_xCuO_4$. While these materials are part of the cuprate family, their crystallographic structures differ from that of LBCO.[7] Thus, LCCO provides the opportunity to study an electron-doped material that is isostructural to LBCO.

We have performed high Q-resolution neutron scattering experiments on high quality LBCO single crystals using the N5 triple axis spectrometer at Chalk River. All measurements were performed using cold neutrons with a fixed final energy of $E_f = 1.2363$ THz (4Å) using flat highly ordered pyrolytic graphite (PG)-002 monochromator and analyser crystals. High-resolution profiles of the elastic magnetic Bragg peaks at and around the (½, ½, 0) position in reciprocal space were measured and their evolution as a function of temperature was tracked. The crystals were aligned in the (H,K,0) scattering plane and cooled using a displex closed-cycle refrigerator with helium exchange gas. In order to achieve high Q-resolution, in addition to using long wavelength neutrons, the beam was very tightly collimated: [open, 0.2°, 0.2°, 1.2°]. A Be filter cooled with liquid nitrogen was used in the main beam to suppress $\lambda/2$ scattering from the high-intensity structural Bragg peak at (1,1,0).

High-resolution reciprocal space maps were made by performing (H,K,0) scans near the (½, ½, 0) magnetic Bragg peak. These maps were used to establish qualitatively the long-range nature of the magnetic order, and to determine the extent of incommensuration at each doping. Order parameter measurements were then taken at several positions on and around the magnetic Bragg position for each sample. The result of these studies is a comprehensive picture of the evolution of magnetic phases in underdoped LBCO.

Figure 1 shows a typical mesh scan for the undoped material with and without the Be filter at T = 3K. Without the filter (Figure 1(a)), four separate peaks are visible close to (½, ½, 0) position. These are due to $\lambda/2$ scattering from the (1,1,0) reflection, with the multiplicity due to the slight orthorhombicity of the LBCO structure and twinning of the crystals. The orthorhombicity produces two peaks for a given Bragg reflection, at higher and lower q corresponding to the a*- and b*- directions, each of which is split into two peaks at equal $|\mathbf{q}|$ due to the sample twinning.

Figure 1(b) shows the same mesh scan repeated with the Be filter in place. With the filter present, only the two peaks at higher $|\mathbf{q}|$ remain, indicating that the magnetic moments point along the b* direction.[8] This mesh scan is typical of those taken for all samples and provides a profile of the magnetic scattering around the (½, ½, 0) position. Similar scans at room temperature, well above T_N in these materials, show a lack of scattering near the (½, ½, 0) position indicating that the

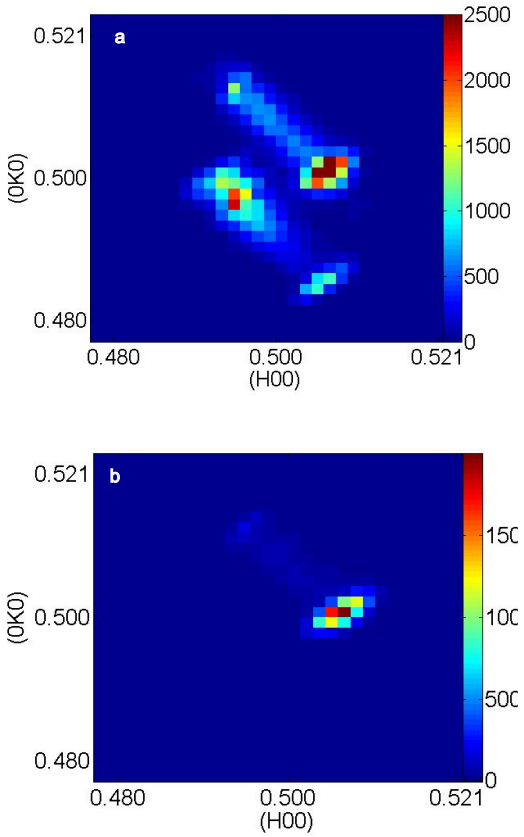

Fig 1. Reciprocal space maps of the magnetic Bragg position in pure La_2CuO_4. Figure 1a) shows a map measured without the use of the Be filter. The higher order ($\lambda/2$) scattering from the (1,1,0) structural Bragg feature can be observed. Figure 1b), shows the mesh scan taken with a Be filter in the incident beam.

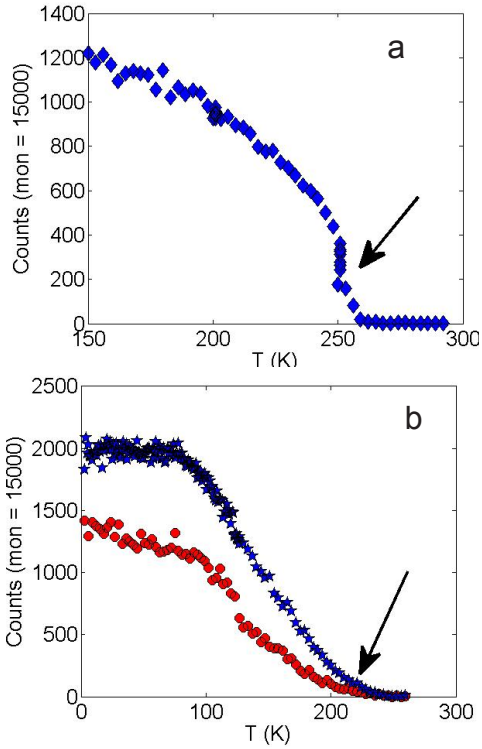

Fig 2. Temperature dependence of the magnetic scattering for a) the pure sample measured at (0.5035, 0.5005, 0) and b) x = 0.006 measured at two distinct reciprocal lattice points close to (½, ½,0) characterizing high intensity and diffuse magnetic scattering at (0.5, 0.508,0) and (0.498, 0.507, 0) are shown. The pure sample shows a well defined 'first-order-like' transition while the 0.6% doped sample shows a gradual increase in magnetic scattering.

scattering seen here is indeed purely magnetic and that the Be filter is very efficient at removing higher order neutrons from the main beam. These profiles were then used to determine appropriate locations for order-parameter-type temperature scans. For each sample, several points on and around (½, ½, 0) reciprocal lattice point were chosen to reflect both long range (high intensity regions) and short range (regions of diffuse scattering) magnetic order in the crystal.

Figure 2(a) shows the average temperature dependence of the magnetic scattering for the undoped sample at all points indicated in Figure 1(b). From this figure, it can easily be seen that the onset of magnetic order occurs at T_N = 250K. Typically in the undoped material, a transition temperature of T_N = 350K is observed.[9] All of our samples, having been grown in a dry O_2 gas environment, contain some excess quantity of oxygen which gives our crystals a chemical formula of the form $La_{2-x}Ba_xCuO_{4+\delta}$ with $\delta > 0$. Excess oxygen introduces holes into the system similar to Ba doping and thus the T_N is lowered considerably in this sample. However, since all samples involved in this study were grown under similar conditions, we expect this effect to be similar across the entire doping range.

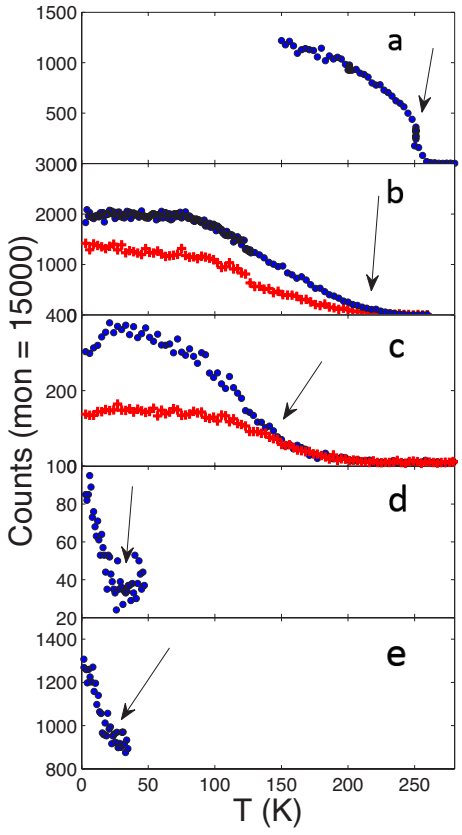

Fig 3. Temperature dependence for: a) pure, b) x = 0.006, c) x = 0.0125, d) x = 0.025 and e) x = 0.035 (data for this sample was taken at HFIR ORNL). T_N (indicated by the arrows) scales inversely with doping.

Figure 2(b) shows the temperature dependence of scattering from two points for the x = 0.006 sample. At this doping, however, there is a clear change in the temperature dependence of the magnetic scattering compared to the pure sample. The addition of a small amount of Ba^{2+} has destroyed the sharp

transition to the AFM state; the magnetism gradually sets in on cooling and only becomes fully developed at ~50K. From this data set, a transition temperature can be inferred by noting the temperature at which sharp, high intensity magnetic scattering departs from the development of less intense, more diffuse peripheral scattering which indicates the disorder caused by Ba doping. Using this method, we have determined the transition temperature for this sample to be $T_N(x = 0.006)$ = 218K. The width of the magnetic peak is quite similar to those of the structural peaks, indicating that the ordering is long-range in nature.

Figure 3 shows the order parameter measurements made for the complete set of LBCO crystals with x = 0, x = 0.006, x = 0.0125, x = 0.025 and x = 0.035, with the vertical lines indicating T_N as determined by the aforementioned method for each sample. Note that as the Ba concentration increases, the disparity between peripheral and intense long range order scattering increases and T_N scales inversely with doping. For the sample with x = 0.0125, the onset of antiferromagnetic order is followed by a re-entrant transition at T = 21K in which ~20% of the 3D order is transformed into 2D order. The drop in scattering intensity is due to the loss of coherence of the antiferromagnetism along the c* direction. This causes the 3D Bragg feature to become 'rod-like' and extend along (0,0,L) (see [10]). For samples with x = 0.025 and x = 0.035 no high intensity magnetic Bragg peak is observed, leaving only diffuse, 2D scattering which is often interpreted as spin-glass like behaviour for LBCO with x > 0.02.[9]

Figure 4 shows our reciprocal space mesh scans for the x = 0.0125 and x = 0.025 samples. In Figure 4(a), the magnetic scattering for the x = 0.0125 sample is shown; despite the oblong shape of the peak due to the mosaic of the crystal, analysis of the peak profile shows that the peak width is reasonably consistent with the width of the structural peak, indicating that, as in lower doping levels, the ordering is long-range in nature. Figure 4(b) shows the difference between magnetic scattering at 50K and at 3K in the x = 0.025 sample; in this sample highly diffuse magnetic scattering is seen, indicating that ordering is short-range in nature with a correlation length of about 14 Å, or about 3 lattice units.

The magnetic phase transitions described above display much of the complexity of the usual x-T phase diagram used to describe the behaviour of high T_c cuprate materials. The various magnetic phases present in LBCO correspond to the electronic phases, including superconductivity, that make this material extremely important in the study of high temperature superconductivity.

The electron-doped material LCCO with x = 0.025 was also included in this study. Although the effects of electron doping are similar to hole doping, excess electrons are less effective at disrupting magnetic order and thus the antiferromagnetic region is much larger in the electron-doped cuprate phase diagram. In addition, electron doping can push these materials into a superconducting phase but this generally requires

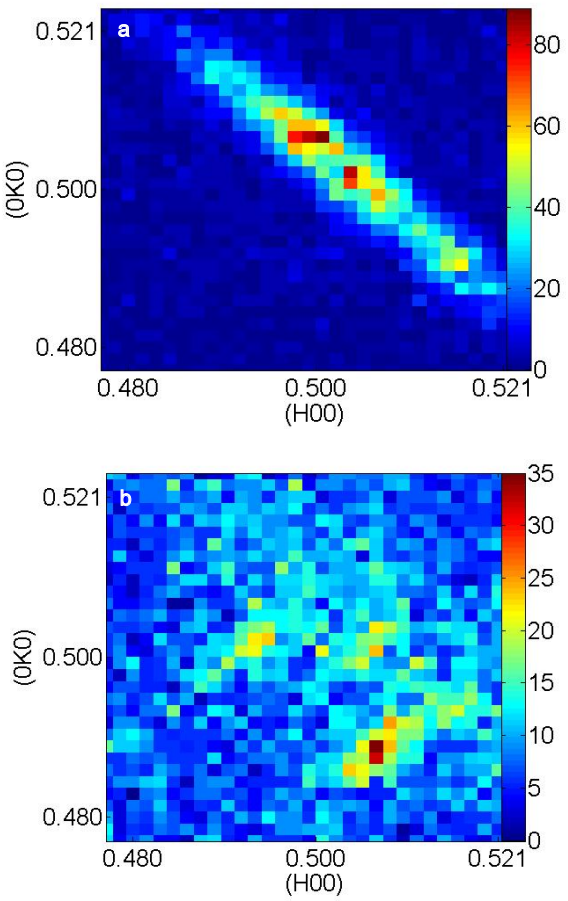

Fig 4. *Reciprocal space mesh scans for the x = 0.0125 (a) and x = 0.025 (b) samples. For the x = 0.0125 sample a comparison of the peak profile shows that the peak width is reasonably consistent with the width of the structural peak, indicating that the ordering is long-range in nature. For the x = 0.025 sample, highly diffuse magnetic scattering is seen indicating that ordering is short-range in nature.*

a much higher concentration than the hole-doped materials. This material has never been studied in high-quality single-crystal form, and preliminary magnetization measurements do not indicate the presence of a superconducting ground state down to 2K. Previous attempts to produce LCCO have met with limited success and have produced materials with a slightly different crystalline structure.[11] Figure 5(a) shows the reciprocal space map taken at T = 3K for LCCO x = 0.025. This crystal shows very little twinning resulting in a better definition of the magnetic Bragg peak compared to the LBCO crystals included in this study. Consistent with other electron-doped cuprates, the introduction of excess electrons has considerably less of an effect on the magnetic order than that of hole doping. While a Ba concentration of 2.5% is well within the spin-glass region, 2.5% Ce doping is well within the antiferromagnetic dome of the electron doped phase diagram.[7] Qualitatively, this can be seen in figure 5(a) by the relatively sharp, high intensity Bragg peak indicating a well-ordered antiferromagnetic state.

The temperature dependence of the magnetic scattering for LCCO with x = 0.025 is shown in figure 5(b). Similar to

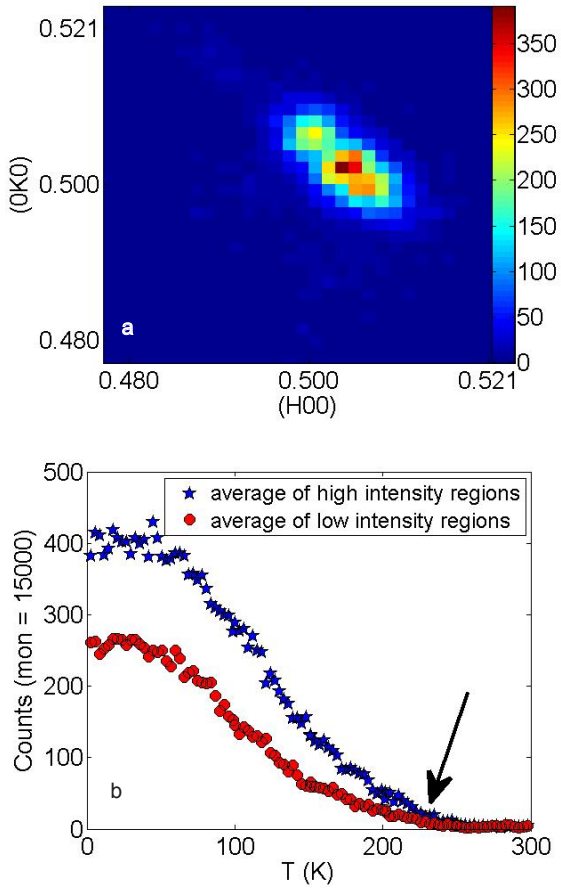

Fig 5. *a) Reciprocal space map of the magnetic Bragg feature in LCCO with x = 0.025. b) Temperature dependence of magnetic scattering for LCCO with x = 0.025. For the higher intensity scattering, the data from (0.5035,0.5035,0) and (0.5050,0.5035,0) were averaged. For the low intensity regions the data from, (0.5005,0.5080,0), (0.5050,0.5050,0) and (0.5080,0.5005,0) were averaged. The gradual transition into the antiferromagnetic state indicates the presence of Ce^{4+} dopant in the crystal.*

LBCO with x = 0.006, the magnetic scattering increases gradually on cooling, in contrast to the sharp, first order-like transition seen in the pure material. While the Bragg feature indicates a well ordered antiferromagnetic ground state, the nature of this transition indicates the presence of the Ce^{4+} dopant in the crystal lattice. From this temperature dependence a Neel-like transition with T_N = 230K can be inferred.

This study confirms the presence of a 3D antiferromagnetic state similar to those in other La-based cuprate high T_C superconducting families. Although the effects of further doping are unknown, our study of LCCO with x = 0.025 confirms that it is possible to dope La_2CuO_4 with Ce^{4+} and that this produces an effect similar to that in other electron doped cuprate materials. We plan to extend our studies of LCCO to higher doping levels in order to explore the nature of electron-doped La_2CuO_4.

Using elastic neutron scattering we have studied the magnetic properties of several single crystals of $La_{2-x}Ba_xCu0_4$ with x < 0.025. A complex magnetic response is found as a function of doping. The undoped parent material exhibits 3D static commensurate antiferromagnetic order. Adding holes into the CuO_2 planes by Ba-doping suppresses this long range 3D AF order to lower temperatures. In addition, starting at x = 0.0125 3D commensurate and 2D incommensurate magnetic orders appear to co-exist at low temperatures. For x = 0.025, no long-range 3D AF order is found and only short range 2D correlations are observed.

References

[1] A. Schilling M. Cantoni J. D. Guo & H. R. Ott, Nature, 363 (1993), 56.
[2] M. K. Wu et al., Phys. Rev. Lett., 58 (1987), 908.
[3] H. Maeda et al., Physica C, 153 (1998), 602.
[4] J. G. Bednorz and K. A. Muller, Z. Phys., 64 (1986), 189.
[5] S. R. Dunsiger et al., Phys. Rev. B, 77 (2008), 224410.
[6] S. R. Dunsiger et al., Phys. Rev. B, 78 (2008), 92507.
[7] Y. Krockenberger et al., Phys. Rev. B, 77 (2008), 060505.
[8] D. Vaknin et al., Phys. Rev. Lett., 58 (1987), 2802.
[9] R.J. Kastner, G. Birgeneau, R. Shirane and Y. Endo, Rev. Mod. Phys., 70 (1998), 897.
[10] G. J. Van Gastel, Z. Yamani, B. D. Gaulin, NRC CNBC Annual Report 2008, (2009), 39.
[11] T. Yamada, K. Kinoshita and H. Shibata, Jpn. J. Appl. Phys., 33 (1994), 168.